Final Report
Refining Hydrocarbon Oxidation Mechanisms via Isomeric Specific Radical Initiated Chemistry

Tracking Number: 2008-93
Grant Activity No. 582-5-64593-FY08-22

Principal Investigator

Simon W. North
Department of Chemistry
Texas A&M University
College Station TX, 77842
swnorth@tamu.edu

Key Personnel

Buddhadeb Ghosh
Department of Chemistry
Texas A&M University
College Station TX, 77842
bghosh@mail.chem.tamu.edu

Summary:

Biogenic emissions are substantial in Eastern and Central Texas, contributing to the regional formation and transport of ozone. Our work has identified and confirmed novel mechanistic pathways in the atmospheric oxidation of isoprene suggesting that current chemistry models of isoprene oxidation may require modification. The impact of this new chemistry on regional ozone may be important and studies to assess and quantify the impact are on-going.

Refining Hydrocarbon Oxidation Mechanisms via Isomeric Specific Radical Initiated Chemistry

Isoprene, 2-methyl-1,3-butadiene, contributes ~44% to annual vegetation emissions. It is the largest single source biogenic VOC emitted worldwide, with an emission rate in excess of ~500 Tg C yr^{-1}. Its lifetime in the atmosphere is approximately 1 hour and is dominated by reaction with hydroxyl radical. Hydroxyl radical initiated photooxidation of isoprene directs much of the ground level ozone production in Texas during summer months. Isoprene oxidation is also thought to contribute to secondary organic aerosol (SOA) formation via further reactions of first-generation end products in both high- and low-NOx conditions and to contribute to hygroscopic SOA formation through cloud processing. The reaction with hydroxyl radical proceeds by electrophilic addition to one of the two double bonds producing four distinct hydroxyalkyl radicals.

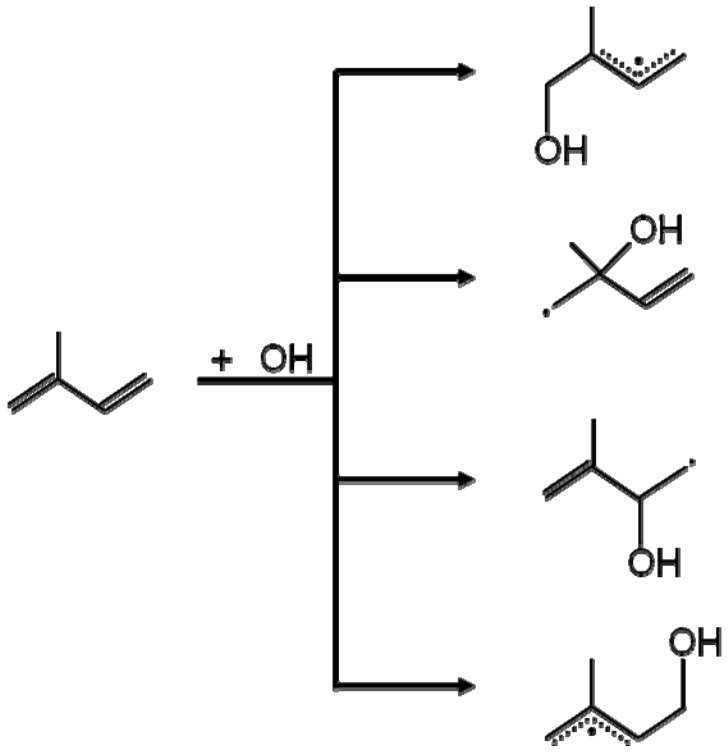

Refining the detailed mechanism of the OH initiated oxidation of isoprene and assessing the accuracy of existing simplified mechanisms, are the focus of current study.

Although significant progress has been made toward unraveling the detailed mechanisms of OH initiated oxidation of isoprene and other unsaturated hydrocarbons, questions persist. In

the case of larger unsaturated hydrocarbons, like isoprene, the electrophilic addition of OH results in multiple radical isomers. Often the number of intermediate species increases following the reaction with O_2 and further branching can occur during subsequent steps on the way to first generation end products. Although recent *ab initio* studies have made a substantial impact in providing *a priori* predictions of these branching ratios in isoprene oxidation, direct experimental confirmation is unavailable. Recent kinetic studies have relied on OH-regeneration to infer information about the isomeric branching. Analysis of the results suggests qualitative agreement with theoretical predictions but the complexity of the reaction systems has precluded a quantitative treatment. To date all of the kinetic data reflects "lumped," non-isomeric selective rate constants.

Direct measurements of the intermediates using either chemical ionization mass spectrometry or transient absorption have also been unable to extract isomeric specific rate constants and branching ratios. Zalyubovsky and co-workers have recently demonstrated the feasibility of using cavity ring-down spectroscopy on the resolved A-X transition of peroxy radicals to obtain selective detection. In those studies, the peroxy radicals were generated *via* reaction of a hydrocarbon with OH in the presence of O_2. As the hydrocarbons become more complex and the resulting number of isomers increases, however, the spectroscopic assignments will be challenging. Ideally one would like to isolate the isomers and thus simplify the ensuing kinetics. In addition to making kinetic studies more tractable, isomeric selective studies permit the investigation of minor, yet important, channels that are difficult to study in the presence of major channel kinetics. The photodissociation of a suitable precursor can, in principle, provide a route to the formation of a single isomer.

Under the current research project we focus on the photolytic production of two possible isomers following OH addition to isoprene, addition of OH to one of the inner carbons and addition to one of the outer carbons. We seek to determine the subsequent kinetics of these isomeric selected intermediates. There are several requirements, which must be considered prior to selecting photolytic precursors for these intermediates: 1) the synthetic preparation of the photolytic precursor should be feasible, 2) the photodissociation should have an appreciable absorption cross-section at the photolysis wavelength and result in a single product channel with near unit quantum yield, 3) the photodissociation should produce intermediates possessing the correct internal energy. The last point is subtle requirement, which is particularly relevant in the present study. The thermal addition of OH to isoprene results in highly activated radicals with internal energies in excess of the exothermicity of the reactions. Thus, in order to mimic subsequent reactivity of these radicals under thermal conditions, the photolytic route must result in a nascent internal energy distribution consistent with thermal activation. Halogenated compounds are suitable precursors since excitation in the UV/Vis region typically involves an $n \rightarrow \sigma^*$ transition on the C-X moiety resulting in prompt dissociation of this bond. Given the relative bond strengths of the carbon-halogen bonds, the location of the corresponding absorption maxima in the UV/Vis region, and the energy partitioning predicted for a direct dissociation on a repulsive potential, we find that the iodine substituted compounds are ideal.

We have selected and prepared the radical precursors for the isomeric isoprene experiments. We have chosen to continue to utilize iodohydrins which were demonstrated to be suitable precursors based on our work on 1,3-butadiene.[1] The iodine-carbon bond is easily

cleaved following an n→σ* transition in the UV near 260 nm yielding the desired OH-adduct. Our first precursor (**1**) yields one of the minor inner isomers (**2**) upon photolysis,

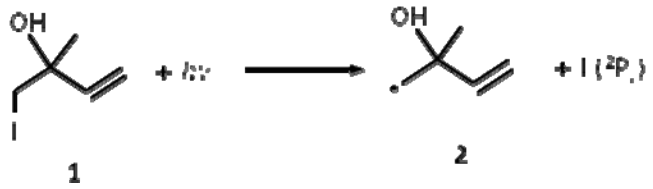

1 2

The synthesis of the 1-iodo-2-methyl-3-buten-2-ol (**1**) is based on the synthetic preparation by Barluenga and co-workers.[2] In a one-pot synthetic preparation, compound (**1**) is prepared in situ via the reaction of hydrogen peroxide with sodium iodide in an acidic, aqueous medium. IOH reacts with unsaturated hydrocarbons via a carbocation intermediate. As such, OH addition to the most highly substituted carbon is favored due to stabilization of the cation. In our synthetic preparation, we find an approximate 5:1 ratio of the reaction product to the minor addition product where IOH adds across the alternative double bond. Purification is achieved *via* column chromatography. Identification and purity of the sample was confirmed by comparison of ^{1}H NMR spectra with the report of Masuda *et al*.[3]

Our second precursor species (**3**) yields the dominant isomer (**4**), formed *via* OH addition to the outer carbon in isoprene in the atmosphere, upon photolysis,

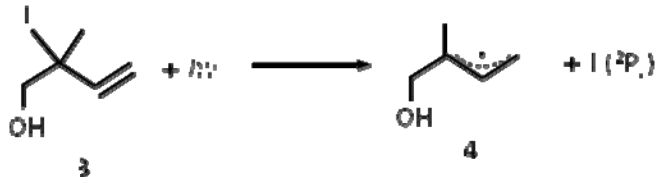

3 4

based on the work of Snider and Duvall.[4] The synthesis involves reaction of isoprene, dissolved in water/acetonitrile, with Ag_2O and I_2 in a molar ratio of 2:1:1. The products were separated by solvent extraction and identified by ^{1}H NMR and Mass Spectrometry. To our knowledge species (**3**) has not been previously reported. A representative ^{1}H NMR Spectrum and Mass Spectrum are provided in the appendix to the report to demonstrate the production of (**3**). Although the synthesis of species (**3**) is more difficult than (**1**) we routinely can produce 1-2 mL of pure sample which is sufficient for our experimental needs.

We have also shown that monodeuteration of the precursor species (**1**) and (**3**) can be achieved by agitating the sample in an ether/D_2O mixture. This permits isotopically labeled kinetic experiments which provide a measure of the intramolecular H-atom transfer pathways. In addition, the gas phase UV/Vis spectra of both samples has been recorded and exhibits the characteristic absorption maximum near 260 nm corresponding to the n→σ* on the C-I moiety. The absorption cross sections at the maxima derived from the spectra are consistent with similar species (approximately 2-4x10^{-20} cm^2). Of future interest is the potential to synthesize iodohydrins of cyclohexadienes which may provide a route to isomeric selective aromatic

chemistry. It should be noted that the synthesis of these species, due to their anti-aromatic nature, *will be considerably more difficult* and will collaboration with synthetic organic colleagues.

Following the synthesis of the iodohydrin precursors we characterized of the photodissociation dynamics of the precursors in order to establish the internal energy distributions of the intermediates. As stated above, the ultimate goal of these studies is not just to generate specific isomeric radicals along the hydrocarbon oxidation pathway, *but to generate these radicals with nascent internal energy that mimics their energy from thermal recombination in the atmosphere*. We have studied the photochemistry given in equations 1 and 2 using velocity-map ion imaging.

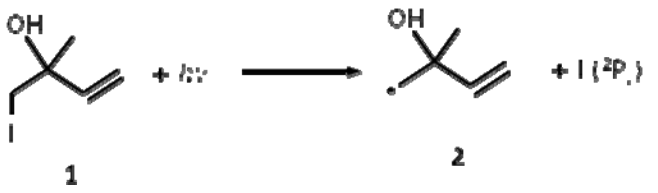

(1)

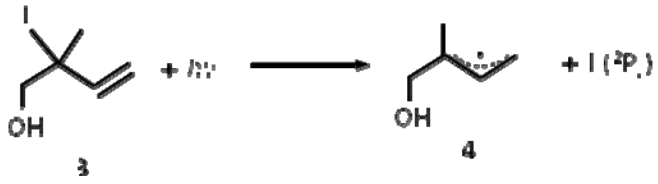

(2)

Our molecular beam apparatus with velocity map ion imaging[5] has been described in the literature.[6] Briefly, a pulsed molecular beam of <1% of the precursor in He (1 atm) was collimated by a conical skimmer and crossed at 90° by the focused output of pulsed dye lasers. Tunable light from two dye lasers is used for photolysis and state-selective ionization of the iodine atom product using 2+1 resonance-enhanced multiphoton ionization (REMPI). The resulting iodine ions were accelerated the length of a 50 cm flight tube and detected by an 40-mm diameter dual microchannel plate (MCP) coupled to a phosphor screen assembly. The Raw photofragment images for I($^2P_{3/2}$) and I($^2P_{1/2}$) arising from the photolysis of precursor **1** at 266 nm are shown in Figure 1. In general, the internal energy distribution of the nascent radicals formed in coincidence with either I or I* products can be obtained from the measured translational energy distributions using energy conservation. The *final radical internal energy distribution*, representing a weighted average of the I and I* components, is shown as the solid line in Figure 1. For comparison a 298 K Boltzmann energy distribution, shifted by the exothermicity of the addition of OH to isoprene to give

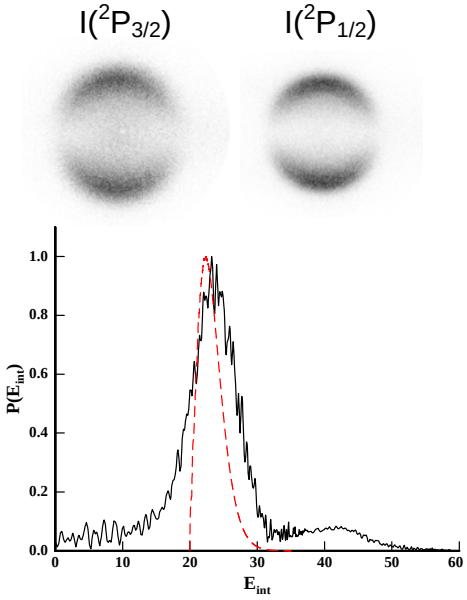

Figure 1. Raw ion images for I($^2P_{3/2}$) and I($^2P_{1/2}$) atoms from the photodissociation of **1** at 266 nm. Nascent radical internal energy distribution (solid line) a 298 K shifted Boltzmann distribution (dashed line).

species **2**, is shown as the dashed line. Such a distribution would be predicted for the 298 K reaction of OH and isoprene in the atmosphere. The distributions are qualitatively similar suggesting that the subsequent kinetics of the radicals produced *via* photolysis should *effectively mimic the radicals formed by thermal recombination*. The internal energy distribution for radical **4**, from the photolysis of precursor **3**, is similar. This result is not surprisingly since the decrease in the C-I bond (due to resonance stabilization of the radical) is offset by the increase in the C-OH bond of the radical. The photodissociation of these species represents an interesting research project in its own right, although not the focus of the current project.

Given the characterization of the photodissociation dynamics, and confirmation of the correct intermediate internal energy the isomeric selective oxidation kinetics studies of isoprene were pursued. We employed the Laser Photolysis/Laser Induced Fluorescence (LP/LIF) technique to probe transient OH radical concentrations in the presence of O_2 and NO. The reaction is initiated by 248 nm photolysis of the precursor **1** or **3**, to yield OH-isoprene adducts **2** and **4.** LIF detection of the OH radicals utilizes excitation on the $Q_1(1)$ transition of the $A \leftarrow X(1,0)$ vibrational band near 282 nm for OH and 287 nm for OD, and collection of the red-shifted fluorescence at 308 nm using a filter. The experimental determination of the pressure and temperature-dependent rate constants is achieved using a recently constructed double-jacketed slow flow apparatus. A high-throughput mechanical pump evacuates a pyrex reaction cell which can be operated over a moderate range of temperatures, monitored using a chromel-alumel thermocouple. Concentrations of O_2, NO, precursor, and Argon buffer gas are controlled by flow meters. All runs were conducted at 298 K and 50 torr total pressure (which ensures that the kinetics are approximately in the 'high-pressure' limit). The delay between photolysis and probe lasers is controlled by a digital delay/pulse generator.

Initial experiments were performed using the photolysis of precursor **1** to generate OH-isoprene adduct **2**. Figure 2 shows OH temporal profiles under 9 different reaction conditions, with respect to concentrations of O_2 and NO, overlaid with kinetics fits of the data. In each of the three panels, a plot of the temporal profiles of OH for three different O_2 concentrations, spanning the range 3.99-16.2 x 10^{14} molecule cm^{-3}, at a constant concentration of NO, is given along with the decay of OH in the absence of O_2 or NO. The top panel displays OH temporal profiles including the varied O_2 concentrations given an NO concentration of 1.08 x 10^{15} cm^{-3}, the middle panel includes the similar results for an NO concentration of 1.62 x 10^{15} cm^{-3}, and the bottom panel displays the results for an NO concentration of 2.16 x 10^{15} cm^{-3}. OH temporal profiles were followed under conditions including NO in the absence of O_2, and including O_2 in the absence of NO, and in both cases, no rise in OH concentrations were observed. In all cases, the model is in excellent agreement with the data. The kinetics mechanism involves 28 reactions although the analysis confirms that the fit is actually highly constrained. Only 6 rate constants were actually adjusted in the fitting procedure. The rate of OH reaction with the iodohydrin precursor was measured employing the LP/LIF technique in our lab yielding a bimolecular rate constant of 1.5 x 10^{-11} cm^3s^{-1}. In addition, for several processes only the relative branching ratios are important and not the absolute magnitudes of the rate constants (due to the rapid timescale). These ratios include the proportion of precursor molecules that undergo photolysis, which is about 0.5% of the total precursor molecule concentration based on the absorption cross section of the iodohydrin and the power density of the laser. A proportion of the nascent β-hydroxyalkyl radicals promptly dissociates to generate an initial concentration of OH.

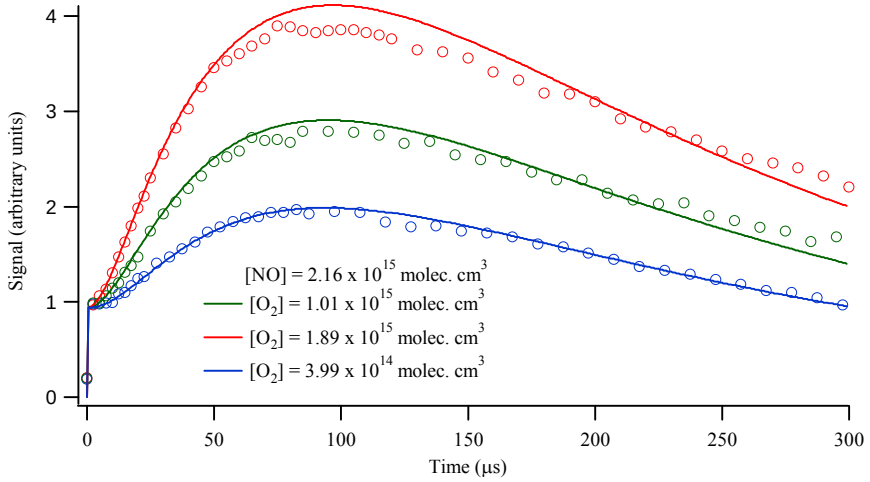

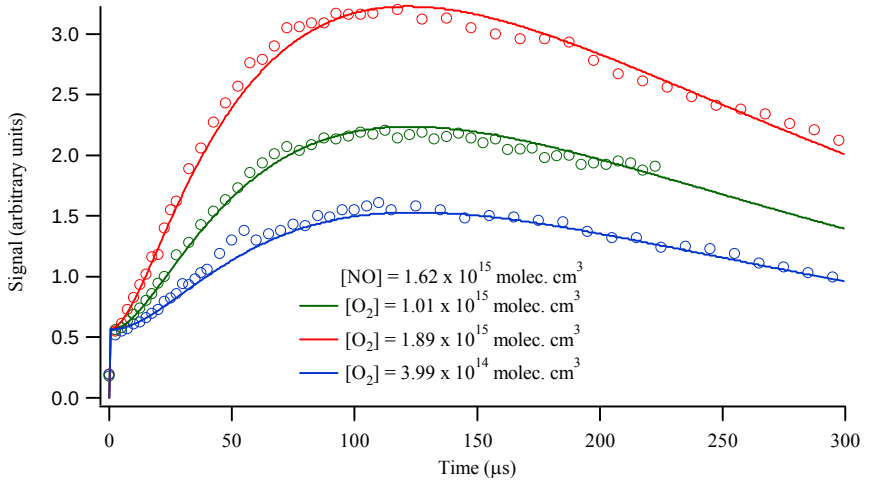

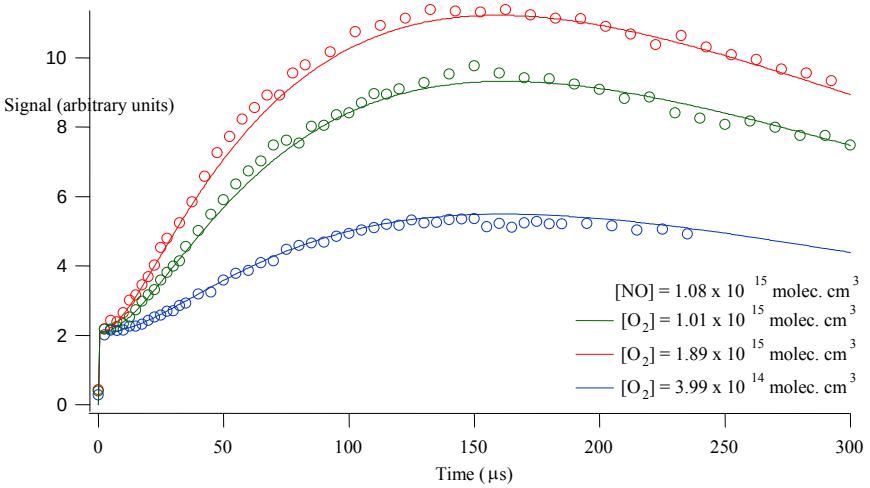

The kinetic model very sensitively depends on the percentage of β-hydroxyalkyl radicals, which promptly dissociate to form OH and isoprene. Figure 3 shows a

kinetics simulation where 34% of the β-hydroxyalkyl radicals undergo prompt dissociation as compared to the similar simulation including 8% prompt dissociation. The larger percent prompt limits the total concentration of hydroxyalkyl radicals available to regenerate OH. This is clearly demonstrated by the much smaller rise of OH compared to prompt OH in the simulation including 34% prompt OH dissociation. As such, our kinetics data indicates that about 8% of the β-hydroxyalkyl radicals will promptly dissociate, which is consistent with the radical internal energy measured in the VELMI experiments and RRKM/ME calculations.

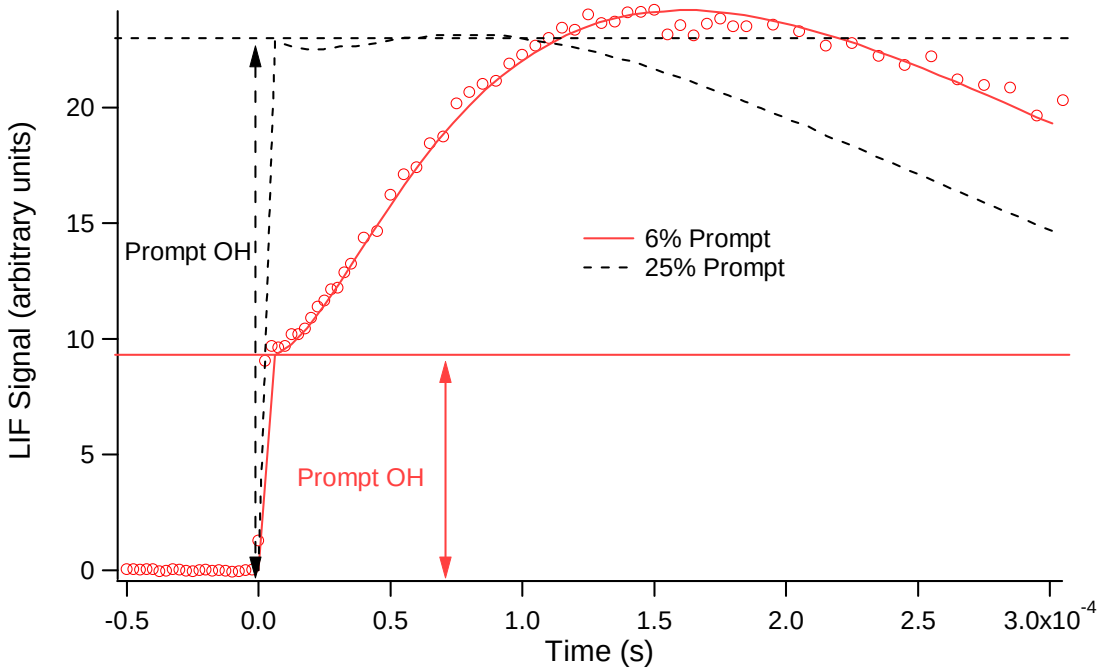

Of the surviving α-hydroxyalkyl radicals, another ratio adjusts the proportion which will cyclically isomerize to form β-hydroxyalkyl radicals to the proportion which collisionally relax into the deep well of the α-hydroxyalkyl adducts. The fates of the α-hydroxyalkyl radicals are either hydrogen abstraction by O_2 or NO termination. The β-hydroxyalkyl radicals are assumed to follow the conventional hydrocarbon oxidation scheme and either undergo NO termination or O_2 addition. Further reactions of the peroxy radicals resulting from O_2 addition to β-hydroxyalkyl radicals ultimately lead to a regeneration of OH radicals, but on a time scale much longer than the observed OH rise in the data. Additional simulations excluding the cyclic isomerization to form α-hydroxyalkyl radicals were performed and it was clear that the time dependence seen in the OH temporal profiles relies on the cyclic isomerization. (not in MCM)

Sensitivity analysis of the modeling was also performed and very few of the 28 reactions had high sensitivity coefficients. Based on this model, the hydrogen abstraction rate from the α-hydroxyalkyl radical is determined to be $(3.72 \pm 0.37) \times 10^{-11}$ cm^3s^{-1}, where the error bars reflect 2 standard deviations from the average. We are also able to establish an α/β branching ratio of 7.0 (*i.e.* 87.5% of the β-hydroxyalkyl radicals isomerize).

We also performed kinetics using the photolysis of precursor **3** to generate OH-isoprene adduct **4**.

Theoretical calculations have predicted that approximately 56% of OH addition to isoprene results in isomer **4** (hydroxyl alkyl radical). The fate of this species is reaction with O_2 to form peroxy radicals (Figure 1). 60% of isomer **4** forms a β-peroxy radical and 40% forms a 1:1 mixture of the (*E*) and (*Z*) forms of δ-peroxy radicals. As show in Figure 1, the β-peroxy radical leads to the formation of methyl vinyl ketone (MVK) which is supported by end-product analysis. The branching ratio of 0.6 for the β-peroxy channel is reasonable given a 8-10% nitrate yield, leads to the formation of ~30% MVK yield which is consistent value for MVK formation from isoprene oxidation. On the other hand, the branching between the (*E*) and (*Z*) forms of δ-peroxy isomers remains untested. The (*E*) and (*Z*) isomers result in hydroxyl carbonyls which have been recently observed using chemical ionization mass spectrometry and may provide closure to the carbon balance.

Figure 4 shows time-dependent OH traces measured at a number of different O_2 concentrations. The precursor concentration was 1.5×10^{13} cm^{-3} and the NO concentration was 1.0×10^{15} cm^{-3}. Based on the kinetic modeling described above we have determined an O_2 addition rate constant, to form the peroxy radicals, of 1×10^{-12} $cm^3 s^{-1}$ and an peroxy + NO rate constant of 8.8×10^{-12} $cm^3 s^{-1}$ which are both consistent with recent theoretical predictions.

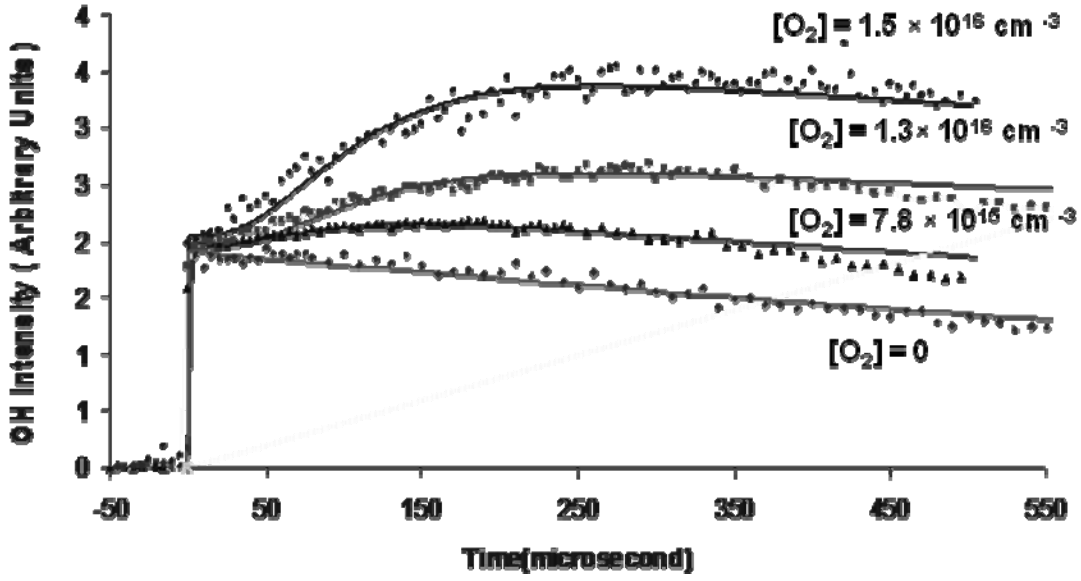

It should be noted that Dibble reported another potential pathway for the (*E*)-OHC_5H_7OH isomer from theoretical studies, which leads to the formation of C_5 di-hydroxyl carbonyl compound. So far, however, no product study has reported the formation of such a compound. Previous interim reports have outlined our isomeric selective OH-cycling experiments to explore

and understand the detailed mechanism associated with the OH-initiated oxidation of the major radical product of OH addition to isoprene. Non-isotopically labeled OH cycling experiments are insufficient to resolve the chemistry associated with the (*E*) form of *δ*-peroxy isomer since all channels ultimately produce OH. For example, the inclusion of the (*E*) channel in our kinetics does not affect appearance of the simulations, *i.e.* we cannot determine the conclude much about the yield of the (*E*) pathway from the cycling experiments.

Isotopically labeled OH cycling experiments, on the other hand, can provide us with insight into the role of the (*E*) peroxy radical channel. If the OH in the precursor molecule is replaced by OD, then both the *β*-hydroxy alkoxy radicals channel and the (*Z*) form of *δ*-hydroxy alkoxy radical channel will lead to the formation of OD. The (*E*) form of *δ*-hydroxyalkoxy radical will result in the formation of OH (Figure 1). Thus, by monitoring the OH radical concentration in an isotopically labeled experiment it is possible to quantify the yield of the (*E*) form of *δ*-hydroxy alkoxy channel. Comparison of the initial prompt rise in the OH fluorescence intensity, due to dissociation, relative to the rise from OH-cycling in experiments using deuterated and the non-deuterated precursors provides a measure of the branching ratio between the (*E*) form of *δ*-hydroxyalkoxy radical and the rest of the hydroxyalkoxy radical.

Our isotopically labeled study has provided the first experimental measurement of the *δ*-hydroxyalkoxy channel with a branching ratio of (20±5)% of the major channel in isoprene oxidation. Since the values of the intermediate rate constants for this major channel are similar to the values obtained for isoprene as a whole, the other major channel, where OH adds to the other end of the carbon chain, is likely to have a similar yield for this channel. This observation validates the previous pathways implicated in the production of hydroxyl-carbonyls in isoprene oxidation.

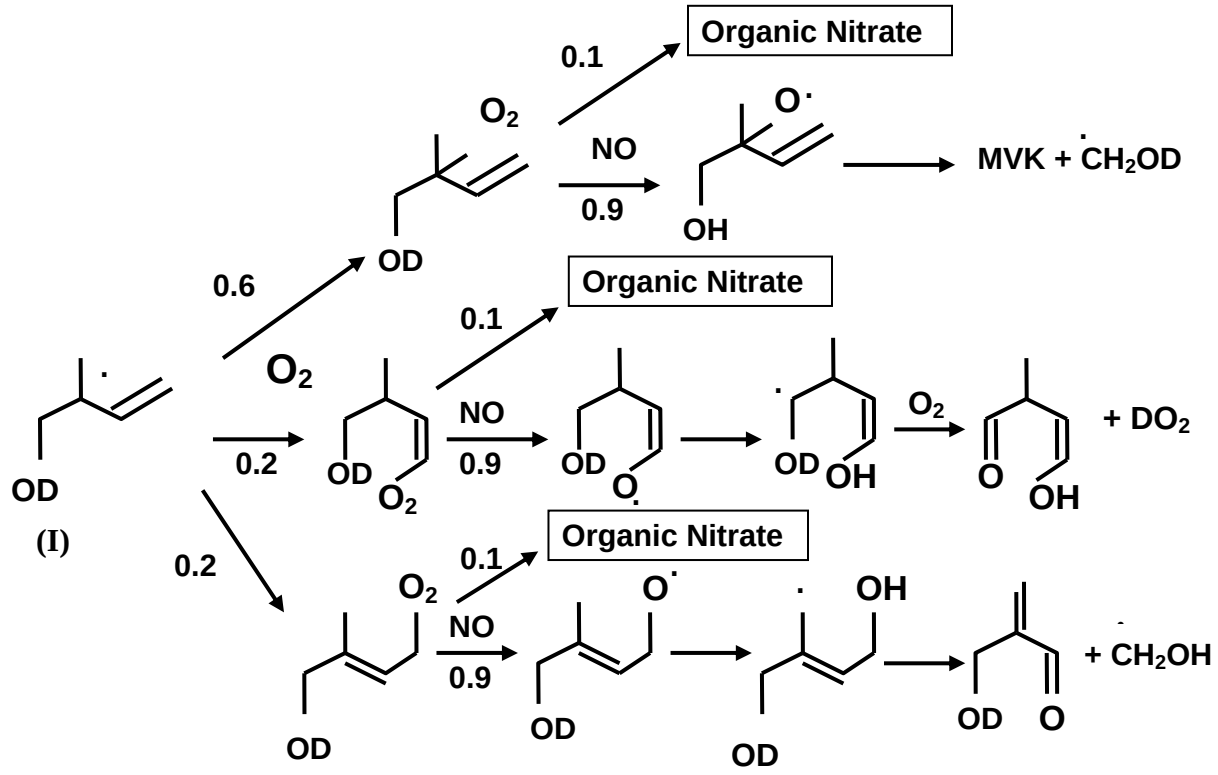

Figure 1. Schematic diagram illustrating the fate of the dominant OH-isoprene adduct.

In conclusion, our work has identified and confirmed novel mechanistic pathways in the atmospheric oxidation of isoprene for the first time. The new chemistry suggests that current models of isoprene oxidation may require modification. The impact of this new chemistry on regional ozone may be important and studies to assess and quantify the impact are on-going. The cyclization reactions, previously overlooked in isoprene chemistry, should occur in many other systems which possess a similar radical/unsaturated motif. In particular, 1,3-butadiene which is an important anthropogenic hydrocarbon emission should exhibit similar chemistry. Based on the results of this study we are optimistic that isomeric selective studies of aromatic species would be feasible. Given the large uncertainties in aromatic oxidation models such studies would provide valuable information for air quality modeling. We would suggest that initial studies on toluene oxidation be pursued.

Appendix

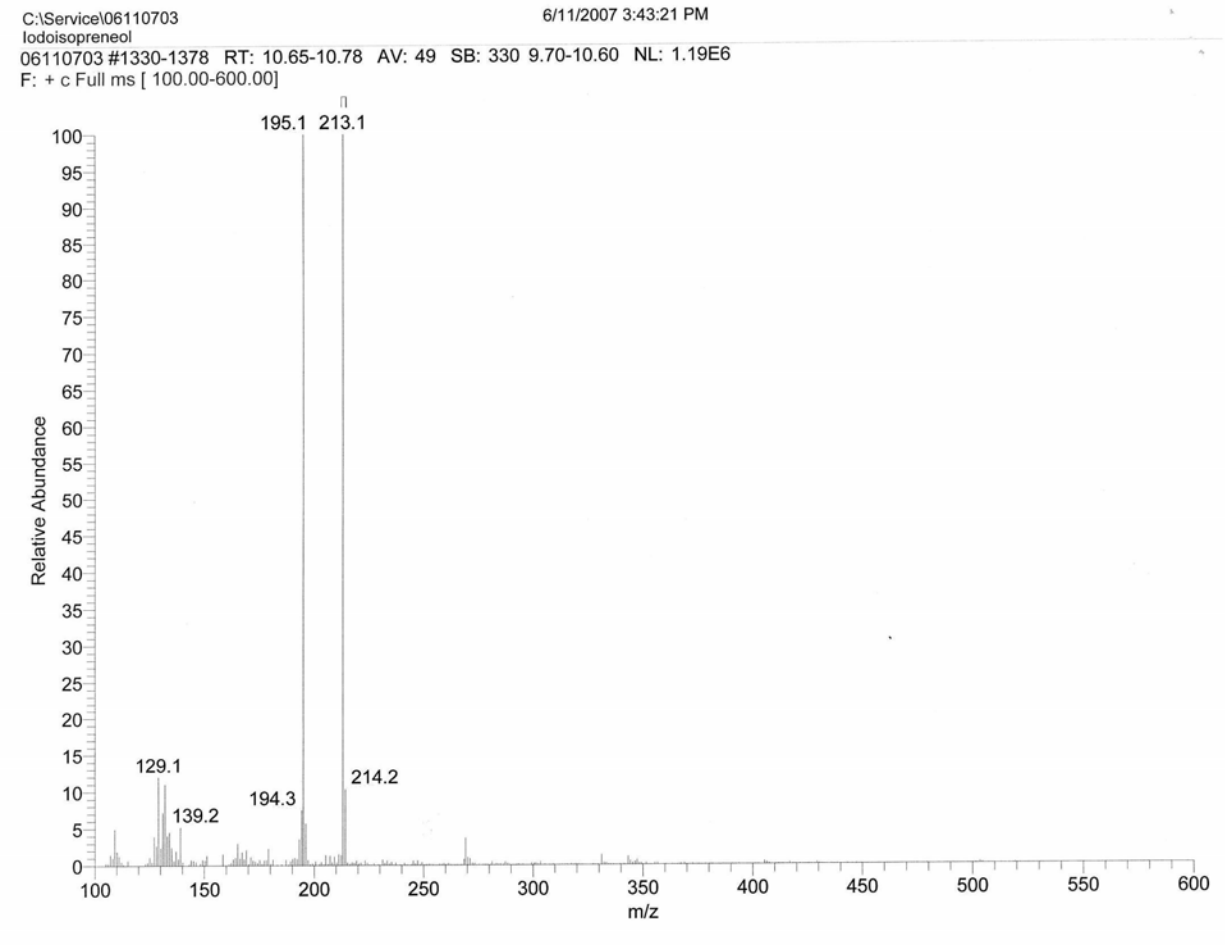

Figure A1. Mass Spectrum of Species **3**. The large peak at *m/z*=213 corresponds to the protonated species and the *m/z*=195 peak to loss of H_2O.

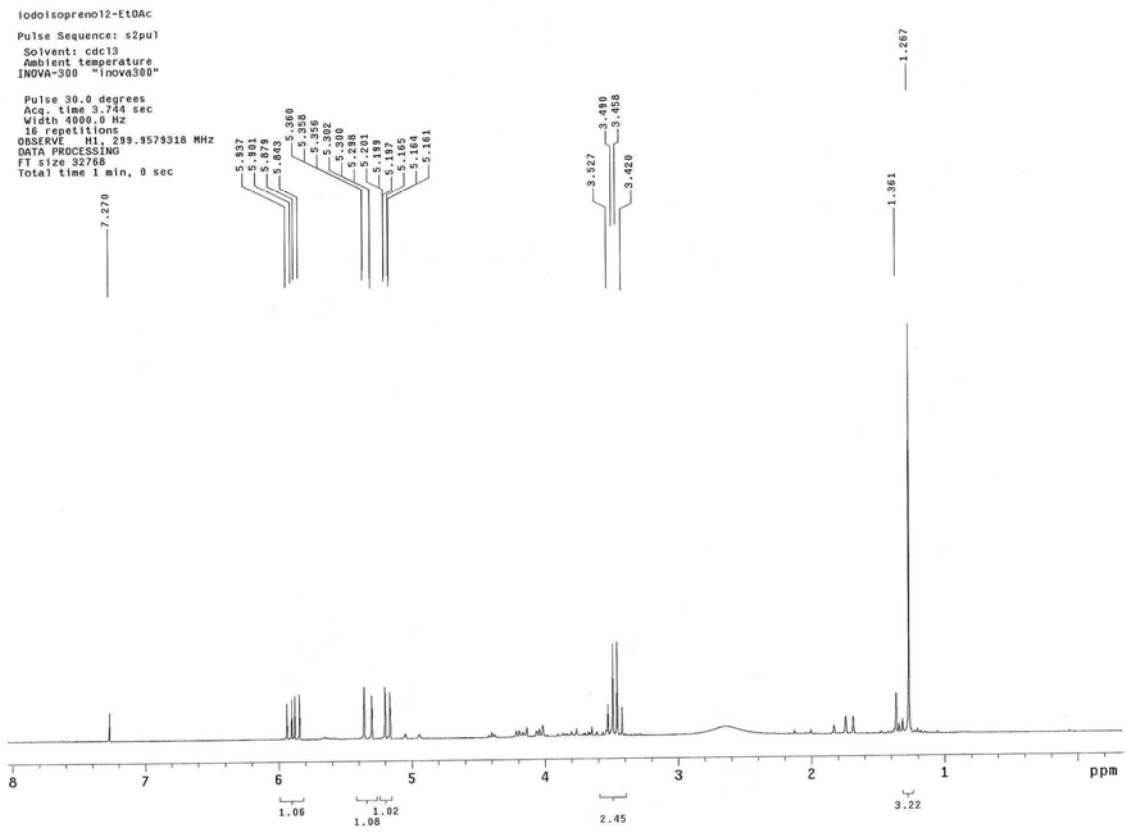

Figure A2. ^{1}H NMR spectrum of species **3**. Only minor solvent peaks are present in addition to peaks associated with the precursor.

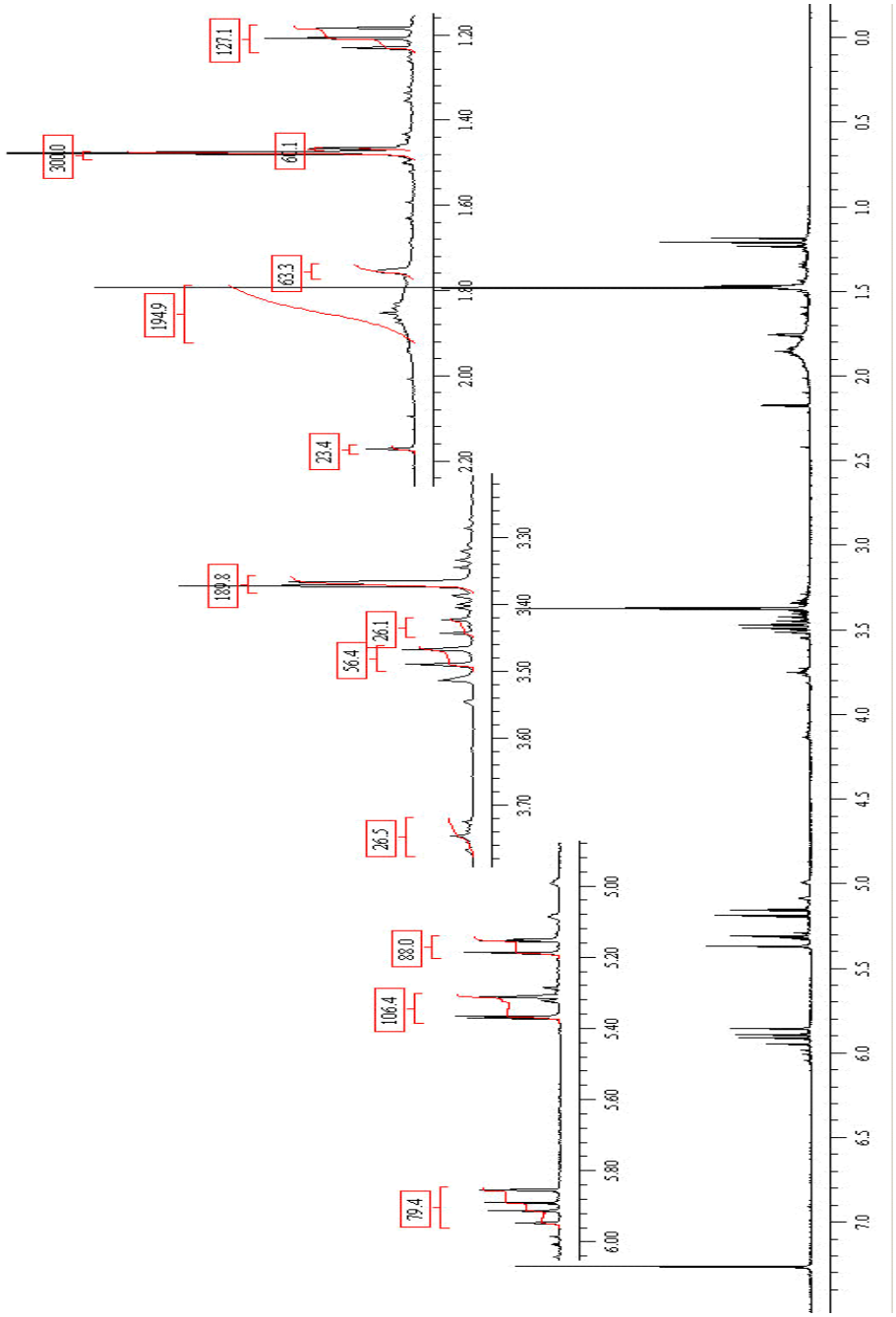

Figure A3. ^{1}H NMR spectrum of species **1**. Only minor solvent peaks are present in addition to peaks associated with the precursor.

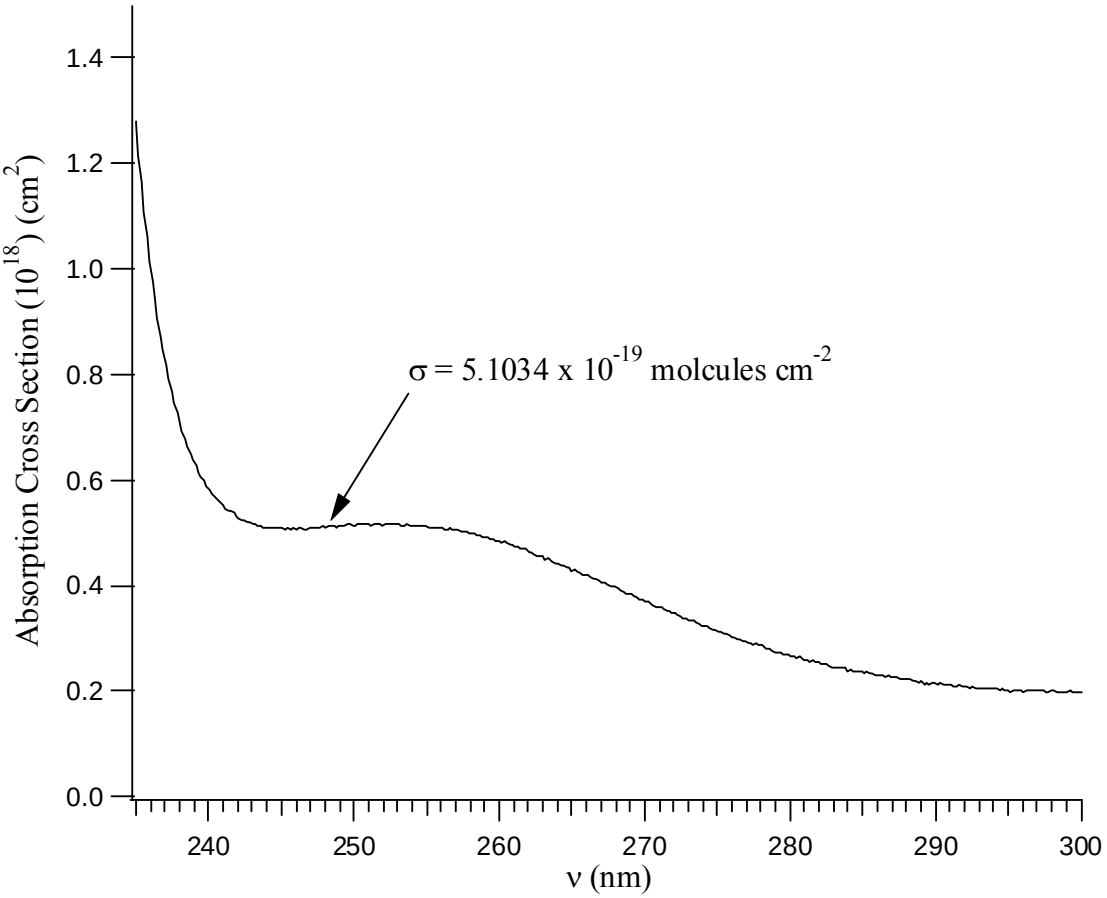

Figure A4. UV-Vis absorption spectrum of species **1**.

References

1 E. E. Greenwald, K. C. Anderson, J. Park, H. Kim, B. J. E. Reich, S. A. Miller, and S. W. North *J. Phys. Chem*. A **109**, 7915 (2005).

2. J. Barluenga, J., M. Marco-Arias, F. González-Bobes, A. Ballesteros, and J. M. González, *Chem. A Eur. J.* **10**, 1677-1682 (2004)

3. H. Masuda, K. Takase, M. Nishio, A. Hasegawa, Y. Nishiyama, and Y. Ishii, Y. *J. Org. Chem.,* **59***,* 5550-5555 (1994).

4 B. B. Snider and J. R. Duvall, *Tetrahedron Lett*. **44**, 3067 (2003).

5. D. W. Chandler and P. L. Houston, "Two-dimensional Imaging of State-Resolved Photodissociation Products Detected by Multiphoton Ionization", *J. Chem. Phys.* **87**, 1445 (1987).

6 H. Kim, J. Park, T. C. Niday, and S. W. North, "The UV Photodissociation Dynamics of ClO Radical using Velocity Map Ion Imaging" *J. Chem. Phys*. **123**, 174303 (2005).